Hindawi
International Journal of Aerospace Engineering
Volume 2022, Article ID 2669954, 13 pages
https://doi.org/10.1155/2022/2669954

Research Article

Application of Gap Metric to LADRC Design in Multilinear Model of SDR

Hongfu Wang[1], **Qinghua Zeng**[1], **An Wang**[2] **and Zongyu Zhang**[1]

[1]*College of Aeronautics and Astronautics, Sun Yat-sen University, Shenzhen, Guangdong Province 518107, China*
[2]*Institute of Air and Space Technology, China Aerodynamic Research and Development Center, Mianyang, Sichuan Province 621000, China*

Correspondence should be addressed to Qinghua Zeng; zqinghua@sysu.edu.cn

Received 26 November 2021; Revised 19 December 2021; Accepted 18 April 2022; Published 6 May 2022

Academic Editor: Maj D. Mirmirani

The solid ducted rocket ramjet (SDR) system faces many disturbances in the process of operation, and the linear active disturbance rejection controller (LADRC) has been widely used in engineering to solve such problems. However, the SDR also has strong nonlinearity, which brings a great challenge to the application of the LADRC in the gas flow regulation of the SDR. And the problem of fast adjustment of the "compensation factor" is one of the main difficulties in LADRC. In this paper, under the LADRC frame, the gas generator system's closed-loop stability of the SDR was analyzed and the range of compensation factors had been calculated, and then, the "gap factor" was introduced and the "cross-iteration" method was used to quickly map out the "compensation factor" in the multilinear model controller based on the variation of the zero-point position of the system and the gap metric between adjacent set points. This greatly simplifies the parameter tuning process of the LADRC when it was applied to strongly nonlinear systems. Finally, through the comparison of simulation with adaptive PI controller and model-assisted LADRC (M-LADRC), the results have shown that the control method designed in this paper can obtain satisfactory performance and has a good engineering application prospect.

1. Introduction

The solid ducted rocket ramjet (SDR) does not need to carry additional oxidizer, and its specific impulse is 3-5 times that of the traditional solid rocket engine, which is an ideal powerplant for supersonic vehicles. While the gas flow regulation technology can realize the adjustable thrust of SDR, this is important for achieving its wide envelope and large maneuverability [1].

With the concerted efforts of many scholars, the gas flow regulation theory of SDR has made certain research progress. Since the gas flow at high temperature and pressure is difficult to measure directly, the common practice is to regulate it indirectly by adjusting the pressure inside the gas generator (GG). Niu et al., for the strong nonlinearity and variable parameter characteristics of the pneumatic gas flow regulation system, proposed a dual-loop control scheme with high gain feedback to suppress nonlinearity, and the experimental results showed a good pressure response [2], but the ultimate purpose of regulating the pressure is to regulate the gas flow, and the pressure-to-flow response process has nonminimum phase (NMP) characteristics, so the pressure regulation loop alone could not completely determine the flow regulation process. In Ref. [3], a new feedback variable was constructed by fusing information from the working pressure of GG and the combustor entrance, which increased the stability margin of the system to some extent. In Ref. [4], an adaptive controller was designed for overcoming the effect of valve friction on the flow regulation process. Reference [5] designed a closed-loop model reference adaptive controller, which could better adapt to the nonlinearity of the pressure regulation system compared to the PI controller and exhibited smaller overshoot during longer and wider range of pressure regulation, but the biggest shortcoming of the paper is its experiments with a cold gas system simulating the GG, which has a large difference between them. So, recent studies have shown the difficulty of gas flow regulation in SDR, on the one hand, due to the strong

nonlinearity and time-varying nature of parameters [6] such as throat area, characteristic velocity of gas, and gas constants in SDR. On the other hand, because there is a NMP characteristic in the response process from GG pressure to gas flow, we cannot focus only on the regulation effect of pressure but also consider the limitation of the undershoot of gas flow.

Active disturbance rejection control (ADRC) technology treats system uncertainties as disturbances and is well adapted to them, so it is still a hot topic of research today. Reference [7] has shown that any linear finite-dimensional controller could be implemented via the LADRC structure, and it is a general-purposed control structure. And the transfer function of LADRC was derived in Ref. [8]. An attitude control method for nonlinear missile system was proposed in Ref. [9], which combined backstepping technique with LADRC. In addition, the LADRC was integrated with U-control theory as an aeroengine speed controller [10]. However, for a system such as SDR, which has strong nonlinearity in addition to uncertainty (the common practice is to make "small perturbation" assumptions and build small perturbation linearization models near the set points), the design and tuning of the control law become complicated and tedious due to the large number of set points. Regarding the parameter tuning problem of LADRC, there are tuning methods based on model information, for example, Ref. [11] used some known disturbances for feedforward compensation, which could reduce the observation burden of linear extended state observer. The third-order LADRC tuning formulas for oscillatory systems were derived from the internal model controllers (IMC) [12]; essentially, it also made use of model information. An actuator model was integrated into the LADRC to improve its performance [13]. And a new tuning method for second-order LADRC based on relay feedback was proposed in Ref. [14]; it also belongs to a model-assisted approach. Fu and Tan proposed a tuning method for reduced-order active disturbance rejection controller (RADRC) using model information as well as the generalized active disturbance rejection control (GADRC) tuning method [15]. However, if the model information is completely unknown then it needs to be identified, such as the forgetting factor recursive least-squares (FFRLS) method used in Ref. [16] and the unscented Kalman filter (UKF) method used in Ref. [17], but it is not suitable for systems with high experimental cost and strong nonlinearity. There are also parameter optimization methods based on intelligent algorithms, for example, the fuzzy control theory was combined with LADRC to adjust the control parameters of LADRC online [18, 19]. Similar LADRC tuning methods are the differential evolution (DE) algorithm designed in Ref. [20], the genetic algorithm (GA) designed in Ref. [21], the particle swarm optimization algorithm (PSO) designed in Ref. [22], the pigeon inspired optimization (PIO) designed in Ref. [23], the simultaneous heat transfer search (SHTS) algorithm designed in Ref. [24], the adaptive algorithm designed in Ref. [25], and the one optimization methods under the constraint of robustness metric described in Ref. [26]. In contrast, Ref. [27, 28] selected suitable parameters according to the frequency domain response under different parameters of LADRC. Since Gao proposed the LADRC [29, 30], the "compensation factor" has become one of the most critical parameters. And Chen also has pointed out that online estimation of the compensation factor is one of the further research directions of LADRC [31].

The gap metric is used to describe the "distance" between two linear systems, and its smaller value indicates that the dynamic characteristics of the two models are closer [32]. Therefore, the method of dividing complex nonlinear systems into multilinear model based on the gap metric theory [33, 34] has been proposed and gradually developed by scholars. However, the partitioning of set points and the design of control laws remain independent of each other. In fact, the variation of the gap metric between linear models largely reflects the variation of the nonlinear system characteristics. Therefore, some design basis of the control law must be included in the gap metric. This paper combined the advantages of the gap metric theory and the LADRC, not only divided the nonlinear model into multilinear model based on the gap metric theory but also introduced the variation of the gap metric among multilinear model into the design and tuning of the LADRC for the first time. The main contributions of this paper are as follows:

(a) The nonlinearity of the GG was analyzed, and the nonlinear model of GG was divided into multilinear model based on the gap metric theory

(b) The stability of GG was analyzed based on Hurwitz theorem in the LADRC control frame, and the range of compensation factors that could stabilize the LADRC was obtained

(c) The compensation factor of the "base point" was calculated based on the root locus method and further mapping the other compensation factors directly based on the gap metric between adjacent set points and the variation of the zero point, which greatly simplifies the design process of the control law and further broadens the application scope of LADRC

(d) The multivariate metrics quantitative analysis method was used to compare the control effects of the three control laws (GM-LADRC, adaptive PI controller, and M-LADRC) and we have analyzed the advantages and disadvantages of the GM-LADRC which was proposed in this paper

The rest of this paper is organized as follows. The mathematical model of SDR and its nonlinear characteristics are described in Section 2, how to divide the nonlinear model into multilinear models based on the gap metric is described in Section 3, and how to calculate the "compensation factor" in LADRC based on the gap metric and the stability analysis of the system are described in Section 4, while the principle of LADRC for gas flow multimodel control is described in Section 5, followed by Section 6, where the three control laws are compared from several aspects, and finally, the conclusion and outlook are given in Section 7.

2. The Mathematical Model and Nonlinear Characteristics of GG

2.1. Mathematical Model of GG. The schematic diagram of SDR is shown in Figure 1. The propellant is burned in the GG to produce primary gas, then the primary gas enters the ram combustor through the throat, and after the secondary combustion occurs with the air flowing into the intake, the gas will be ejected through the nozzleless booster to produce thrust. The ratio of air to (primary) gas is different (air-fuel ratio), the degree of combustion will be different, and the thrust generated also would be different, so in order to make the ramjet generate different thrust, it is necessary to regulate the mass flow of primary gas. Since the mass flow rate of high temperature and pressure gas is not easily measured directly, so it is generally controlled indirectly by controlling the pressure in the GG. We can change the area of the GG throat by means of the interstage valve, which in turn will cause a change in the working pressure of the GG and a further change in the combustion rate of the propellant; finally, the mass flow rate of gas (abbreviated as gas flow) would be changed.

The basic principle of the GG mathematical model is the law of "mass conservation," which means that the mass of gas generated by the combustion of propellant is equal to the sum of the mass of the gas inside the GG and the mass of the discharge from the throat. In this paper, we follow the mathematical model of GG established in Ref. [35], and the dynamic equilibrium differential equation within GG can be expressed in the form of

$$\frac{dP_g}{dt} = \frac{R_g \cdot T_g}{V} \cdot \left(\rho_b \cdot A_b \cdot a \cdot {P_g}^n - \frac{P_g \cdot A_t}{C_r}\right), \tag{1}$$

where P_g is the gas pressure in GG, R_g is the gas constant, T_g is the gas temperature, and V represents the free volume, which means the volume between the propellant end face and the throat. ρ_b represents the propellant density, A_b represents burning area of the propellant, a represents the propellant combustion rate coefficient, n represents the pressure index, A_t represents the throat area, C_r represents the characteristic velocity of the gas, and θ represents the swing angle of the interstage valve.

If the transfer function from A_t to θ is denoted by K_θ, then the transfer functions from P_g and m_g to θ could be expressed in the form of equations (2) and (3). (See part A in Supplementary Materials for score analysis.)

$$\frac{\Delta P_g(s)}{\Delta\theta(s)} = \frac{-K_1(t)}{s + T_1(t)}, \tag{2}$$

$$\frac{\Delta \dot{m}_g(s)}{\Delta\theta(s)} = \frac{K_2(t) \cdot s - K_3(t)}{s + T_1(t)}, \tag{3}$$

where

$$\begin{aligned}
T_1(t) &= -\frac{R_{g0}(t) \cdot T_{g0}(t)}{V_0(t)} \cdot \left[\rho_b \cdot A_b \cdot a \cdot \left(1e^{-6}\right)^n \cdot n \cdot P_{g0}(t)^{(n-1)} - \frac{A_{t0}(t)}{C_{r0}(t)}\right],\\
K_1(t) &= K_\theta(t) \cdot \frac{R_{g0}(t) \cdot T_{g0}(t)}{V_0(t)} \cdot \frac{P_{g0}(t)}{C_{r0}(t)},\\
K_2(t) &= K_\theta(t) \cdot \frac{P_{g0}(t)}{C_{r0}(t)},\\
K_3(t) &= \frac{K_1(t) \cdot A_{t0}(t) - P_{g0}(t) \cdot T_1(t) \cdot K_\theta(t)}{C_{r0}(t)}.
\end{aligned} \tag{4}$$

2.2. Mathematical Model of Interstage Valve. To make the study more convenient, the mathematical model of the interstage valve (also known as the valve motor) can be identified and equated to a second-order system by a frequency response test. As shown in Figure 2, the resonant frequency (ω_r) of the valve motor is about 65.94 rad/s and the high resonance peak ($L(\omega_r)$) is about 1.722 dB, which can finally be derived as its equivalent second-order transfer function according to equation (5), and the result is shown in equation (6).

$$\begin{cases}
\omega_r = \omega_n \bullet \sqrt{1 - 2\bullet\xi^2},\\
M_r = A(\omega_r) = \dfrac{1}{2\bullet\xi\bullet\sqrt{1-\xi^2}},\\
20\bullet\log_{10}A(\omega_r) = L(\omega_r).
\end{cases} \tag{5}$$

The solution is $\xi = 0.46$ and $\omega_n = 87.34$.

$$G_v(s) = \frac{{\omega_n}^2}{s^2 + 2\bullet\xi\bullet\omega_n\bullet s + {\omega_n}^2} \approx \frac{7628}{s^2 + 80.35\bullet s + 7628}, \tag{6}$$

where ξ represents the damping ratio and ω_n represents the undamped natural frequency. ω_r represents the resonant frequency, and M_r represents the resonant peak.

2.3. Nonlinearity of GG. During the pressure response within the GG, the values of P_{g0}, V_0, A_t, C_r, R_g, and T_g vary with the operating conditions of the GG in equation (2), which eventually leads to the nonlinear changes of K_1 and T_1. Taking an SDR ground test as an example, the values of K_1 and T_1 can be calculated based on the set points on the pressure response curve and the system parameters at the set points. As shown in Figure 3, it could be seen that K_1 and T_1 exhibit a strong nonlinear with the change of pressure.

3. Determining Multilinear Models with Gap Metric

The gap metric is used to characterize the distance between two linear systems, and its value ranges from 0 to 1. The smaller the value is, the closer the dynamic characteristics of the two systems are. According to the description in Ref. [32], the design of the gap threshold was subjective. In this paper, the average change rate of the open-loop gain (K_1

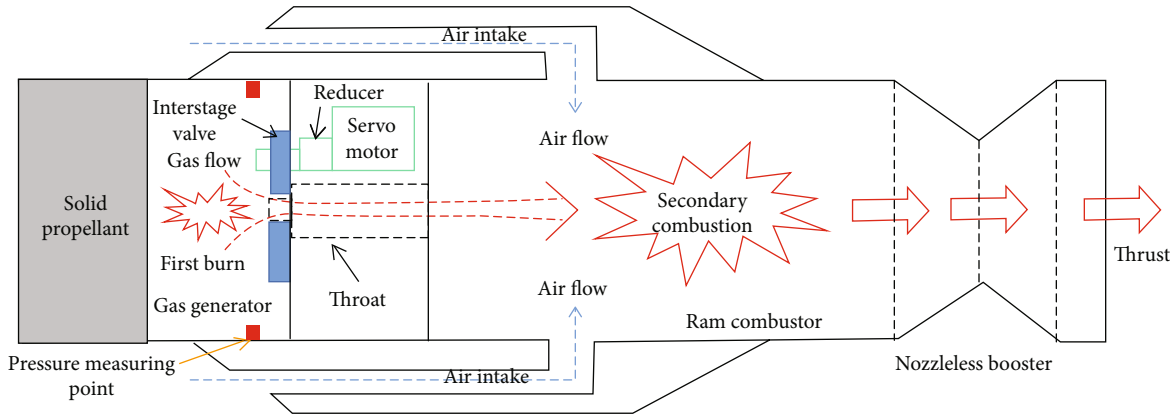

Figure 1: Schematic structure of the SDR.

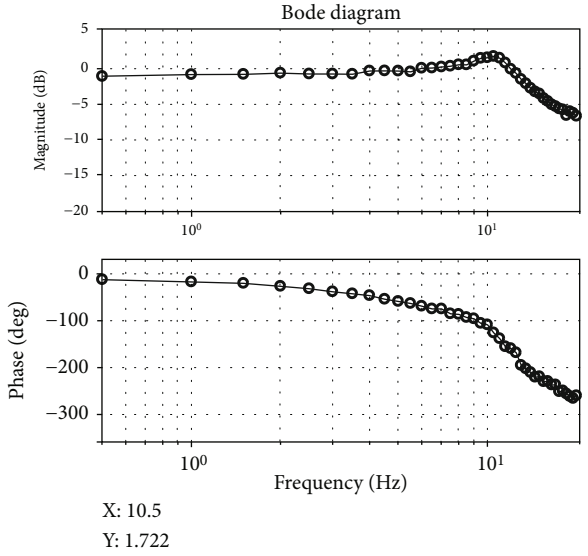

Figure 2: Frequency response of the valve motor.

/T_1) and the time constant ($1/T_1$) between adjacent set points could be kept within 20%, so the gap threshold was set as 0.05. And the set points with the gap metric less than this threshold were clustered, which was used as a basis to obtain the linear model bank of the system. Figure 4(a) indicates the gap between adjacent set points when the free volume is constant but the pressure varies. And Figure 4(b) shows the gap between adjacent set points when the pressure is constant but the free volume varies. If P_1 and P_2 are two scalar transfer functions, then the gap value of the *Vinnicombe* method is calculated according to [36]

$$\delta_v(P_1, P_2) = \sup_{\omega \in R} \frac{|P_1(j\omega) - P_2(j\omega)|}{\sqrt{1 + |P_1(j\omega)|^2} \bullet \sqrt{1 + |P_2(j\omega)|^2}}. \tag{7}$$

For the present system, assuming that the systematic parameters of the adjacent set points are K_{1N} and T_{1N}, the expression can be further written as

$$\begin{cases} \delta_v(P_1, P_2) = \max\left(\sqrt{\dfrac{B}{D}}, \sqrt{\dfrac{A^2 \bullet M}{(M-B)\bullet(M-B+A\bullet C)+A^2\bullet D}}\right), & A\bullet D \geq B\bullet C, \\ \delta_v(P_1, P_2) = \sqrt{\dfrac{B}{D}}, & A\bullet D < B\bullet C, \end{cases} \tag{8}$$

where

$$\begin{aligned} A &= (K_{1N} - K_1)^2, \\ B &= (K_{1N}\bullet T_1 - K_1 \bullet T_{1N})^2, \\ C &= T_1{}^2 + K_1{}^2 + T_{1N}{}^2 + K_{1N}{}^2, \\ D &= \left(T_1{}^2 + K_1{}^2\right)\bullet\left(T_{1N}{}^2 + K_{1N}{}^2\right), \\ M &= \sqrt{B^2 + A\bullet(A\bullet D - B\bullet C)}. \end{aligned} \tag{9}$$

The final division results are shown in Figure 5. Compared with the traditional "equal interval" division method, the 10 pressure points and 10 free volume points (100 set points in total) were selected for designing the control law of the flow regulation system.

Immediately, the change in the characteristics of the system was analyzed by calculating the system parameters under the above set points. Figure 6 represents the variation law of the system parameter K_3 to K_2 ratio, which determines the position of the system's zero point; the smaller the value, the closer it is to the imaginary axis, the greater the undershoot. Under the same pressure condition, the value gradually decreases with the increase of free volume, and under the same free volume condition, the value also gradually decreases with the increase of pressure. This is the inherent characteristic of the system; in order to make the undershoot of the flow response not too large, it is necessary to limit the response rate of the flow according to the changes in pressure and free volume and must not only focus on the response of the pressure alone.

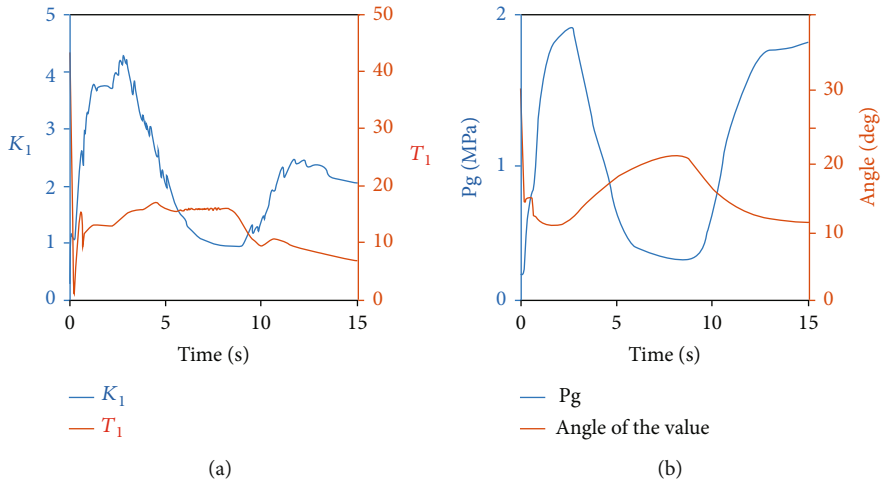

FIGURE 3: Variation of system's parameters in a ground test. (a) Variation of K_1 and T_1 in a ground test. (b) Variation of P_g and the angle of valve in a ground test.

4. A "Compensation Factor" Mapping Method Based on Gap Metric and Stability Analysis

LADRC has the advantages of simple structure and easy implementation, thus making ADRC break through the bottleneck of parameter rectification and engineering. The basic idea of the LADRC algorithm is to linearize the expanded state observer (ESO) and associate its parameters with the observer bandwidth. For a first-order system, the ESO could be written as equation (10). And the expression of the control law could be written as equation (11). (See part B in Supplementary Materials for score analysis.)

$$\begin{cases} \dot{z}_1 = \beta_1 \cdot (y - z_1) + z_2 + b_0 \cdot u, \\ \dot{z}_2 = \beta_2 \cdot (y - z_1), \end{cases} \tag{10}$$

$$u = \frac{(\omega_c \cdot (R - z_1) - z_2)}{b_0}, \tag{11}$$

where $\beta_1 = 2 \cdot \omega_0$ and $\beta_2 = \omega_0{}^2$. z_1 and z_2 are the outputs of ESO, ω_c is the controller bandwidth, and ω_0 is the ESO bandwidth. y is the system output, which is equivalent to the pressure of GG, and R is the input of the linear state error feedback (LSEF).

Since the response bandwidth of the interstage valve angle is much larger than that of the gas flow response, the valve motor loop can be temporarily treated as an ideal link in the control law design stage to reduce the computational effort, and then, it should be introduced to check the stability of the whole system when the control law design is completed. Similarly, the closed-loop transfer function of the system for the reduced-order ESO (without neglecting the observer error) could be obtained as shown in equation (12) by the method discussed in Ref. [37] (see part C in Supplementary Materials for score analysis.), and the equivalent structural block diagram of the system including LADRC and GG is shown in Figure 7. In this paper, the disturbed state of the system was also considered.

$$G_{cl}(s) = \frac{\omega_c \bullet G_1(s) \bullet G(s)/b_0}{1 + G_1(s) \bullet G(s) \bullet H(s)/b_0}, \tag{12}$$

where

$$\begin{aligned} H(s) &= \frac{\omega_c \bullet \left(\omega_0{}^2 + 2\omega_0 \bullet s\right) + \omega_0{}^2 \bullet s}{(s + \omega_0)^2}, \\ G_1(s) &= \frac{(s + \omega_0)^2}{s^2 + (2\omega_0 + \omega_c) \bullet s}, \\ G(s) &= \frac{K_1 + \Delta K_1}{s + (T_1 + \Delta T_1)}. \end{aligned} \tag{13}$$

If $\omega_0 = P \bullet \omega_c$, then equation (12) can be further written in the form of

$$G_{cl}(s) = \frac{\omega_c \bullet K_1 \bullet (s + P \bullet \omega_c)^2}{a_3 \bullet s^3 + a_2 \bullet s^2 + a_1 \bullet s + a_0}, \tag{14}$$

where

$$\begin{aligned} a_3 &= b_0, \\ a_2 &= b_0 \bullet [(T_1 + \Delta T_1) + (2P + 1) \bullet \omega_c], \\ a_1 &= b_0 \bullet (2P + 1) \bullet \omega_c \bullet (T_1 + \Delta T_1) + (K_1 + \Delta K_1) \bullet \left(P^2 \bullet \omega_c{}^2 + 2P \bullet \omega_c{}^2\right), \\ a_0 &= (K_1 + \Delta K_1) \bullet P^2 \bullet \omega_c{}^3. \end{aligned} \tag{15}$$

It is well known that Lyapunov has proved the remarkable conclusion that if the linear approximation of a system is strictly stable, then the nonlinear system will be stable in some domain at the equilibrium point where the linear approximation is applied. Therefore, according to the Hurwitz theorem, the sufficient condition for the

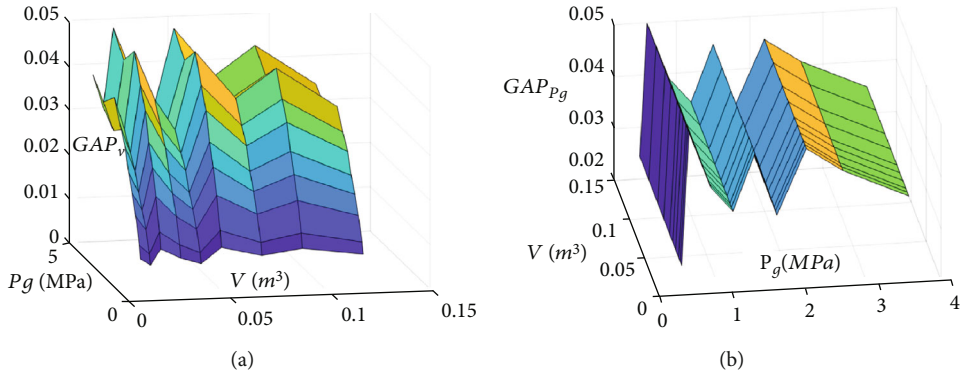

Figure 4: Gap metric between adjacent set points. (a) The gap between adjacent set points when the free volume is constant but the pressure varies. (b) The gap between adjacent set points when the pressure is constant but the free volume varies.

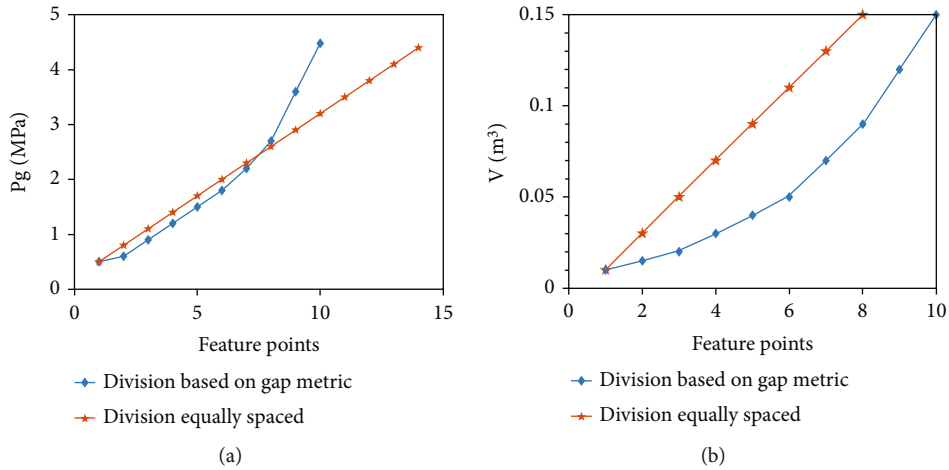

Figure 5: The set point classification based on gap metric. (a) The 10 selected pressure set points. (b) The 10 selected free volume set points.

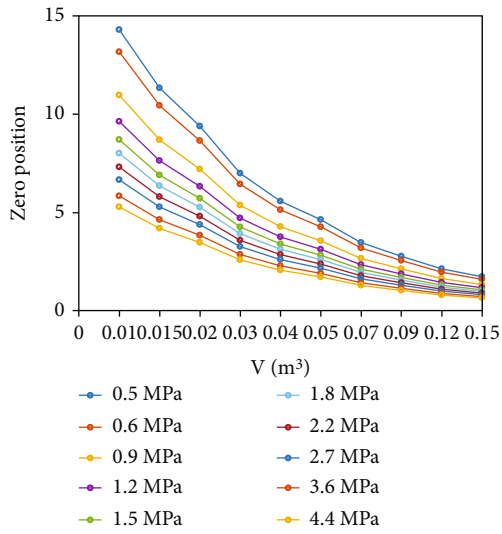

Figure 6: The variation law of system's zero position.

system to be stable at each equilibrium point could be found in

$$\begin{cases} b_0 > 0, \\ T_1 + \Delta T_1 > 0, \\ K_1 + \Delta K_1 > 0, \\ \omega_c > \dfrac{1}{8} \bullet (T_1 + \Delta T_1). \end{cases} \tag{16}$$

For this system, the value of the system parameter T_1 at the selected set points will not exceed 50. Although ω_c taken large enough could satisfy the stability condition, but too large ω_c would affect the dynamic characteristics of the system and reduce the convergence speed of the system. Therefore, comprehensive consideration was made so that $P = 2$ and $\omega_c = 10$ rad/s.

In this paper, the "base point" was defined as the starting set point of the control law design, while the control parameters of other set points should be mapped under the premise of ensuring the stability of the system, relying on the

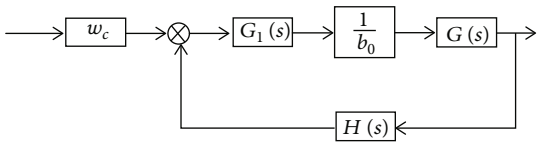

Figure 7: Equivalent structure diagram of the system containing LADRC and GG.

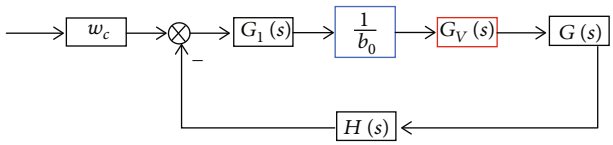

Figure 8: Equivalent structure of the system considering the actuator.

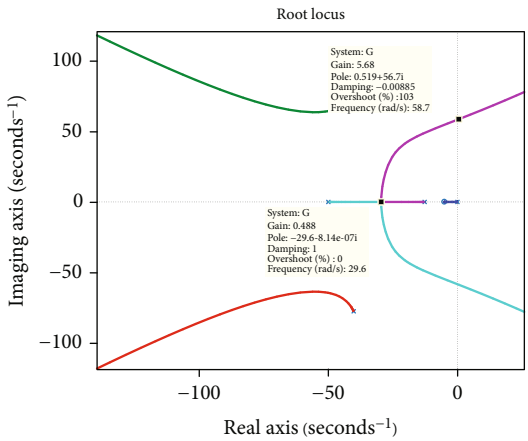

Figure 9: The root locus of the system at the base point.

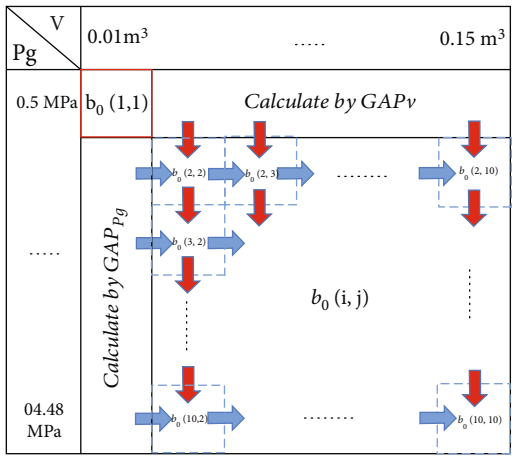

Figure 10: Calculation method of compensation factor.

gap metric between adjacent set points and the control parameters of the "base point." The set point which could make the system's "zero-pole point" closest to or farthest from the imaginary axis should be selected as the "base point," with the aim of ensuring that the control parameters

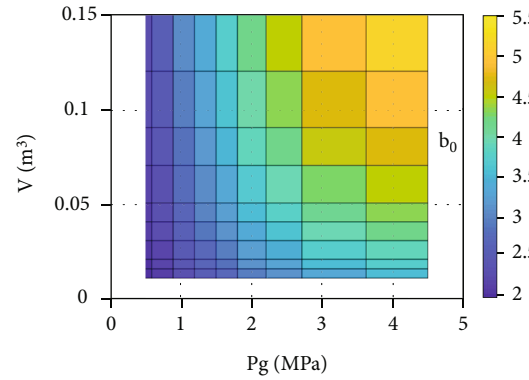

Figure 11: Calculation results of compensation factor.

are monotonic over as large a range as possible. For example, for a system with N-dimensional set points, assuming that the control parameter at the "base point" is $K(i_*, j_*, k_*, \cdots)$, the mapping rules for the control parameters at other set points could be performed as in

$$K(i,j,k,\cdots) = f(U_A(i,j,k,\cdots), U_B(i,j,k,\cdots), U_C(i,j,k,\cdots),\cdots), i \neq i_* \| j \neq j_* \| k \neq k_* \cdots, \tag{17}$$

where $U_A(i,j,k,\cdots) = g(K(i \pm 1, j, k, \cdots), \mathrm{GAP}_A(i \pm 1, j, k, \cdots), \cdots), i, j, k, \cdots \in N^*$ and $i \neq i_*$.

$U_B(i,j,k, \cdots) = g(K(i, j \pm 1, k, \cdots), \mathrm{GAP}_B(i, j \pm 1, k, \cdots), \cdots), i, j, k, \cdots \in N^*$ and $j \neq j_*$.

$U_C(i,j, k, \cdots) = g(K(i, j, k \pm 1, \cdots), \mathrm{GAP}_C(i, j, k \pm 1, \cdots), \cdots), i, j, k, \cdots \in N^*$ and $k \neq k_*$.

$U_A(i,j,k,\cdots)$, $U_B(i,j,k,\cdots)$, and $U_C(i,j,k,\cdots)$ denote the control parameters calculated iteratively along different dimensions, respectively.

For the gas flow response of GG, in which undershoot is a stronger constraint, so the set point at $P_g = 0.5$ MPa and $V = 0.01\ \mathrm{m}^3$ was selected as the "base point," whose zero point in the right half-plane is the farthest from the imaginary axis, and $b_0(1,1)$ is the compensation factor at the "base point." As shown in Figure 8, after considering the valve motor model, the compensation factor of the "base point" could be calculated by the points on the system's root locus. As shown in Figure 9, if the gain point is chosen to be 0.5, the value of $b_0(1,1)$ is the reciprocal of the gain, so its value is 2. Since $b_0 \propto K_1 \propto \delta_v(P_1, P_2)$, the compensation factor could be considered positively correlated with gap metric and could be calculated as in

$$b_0(i,j) = \max\left(b_V(i,j), b_{P_g}(i,j)\right), \tag{18}$$

where $b_{P_g}(i,j) = b_0(i-1,j) + K \bullet \mathrm{GAP}_{P_g}(i-1,j)$, $i \in [2, 10], j \in [1, 10]$.

$b_V(i,j) = b_0(i, j-1) + K \bullet \mathrm{GAP}_V(i, j-1)$, $i \in [1, 10], j \in [2, 10]$.

i and j are the number of rows and columns in the set point table, respectively. From equation (18), we can see that when $i = 1$, $b_0(i,j)$ is uniquely determined by $b_V(i,j)$. And

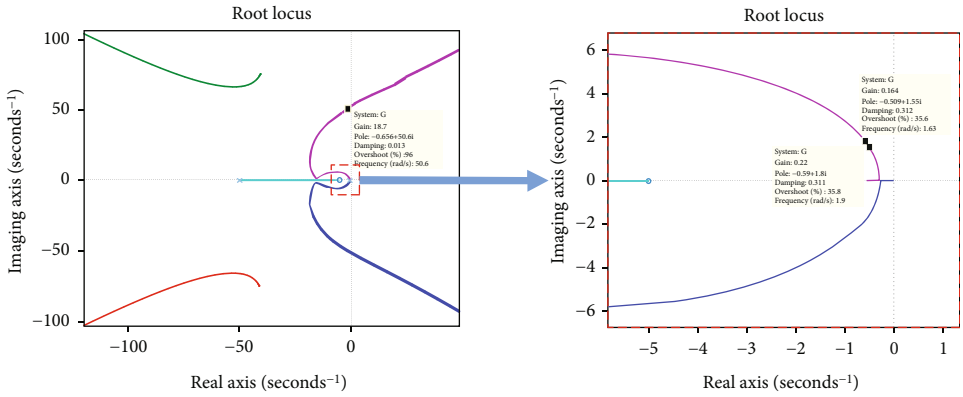

Figure 12: The root locus of the set point at $P_g = 4.48$ MPa and $V = 0.15$ m^3.

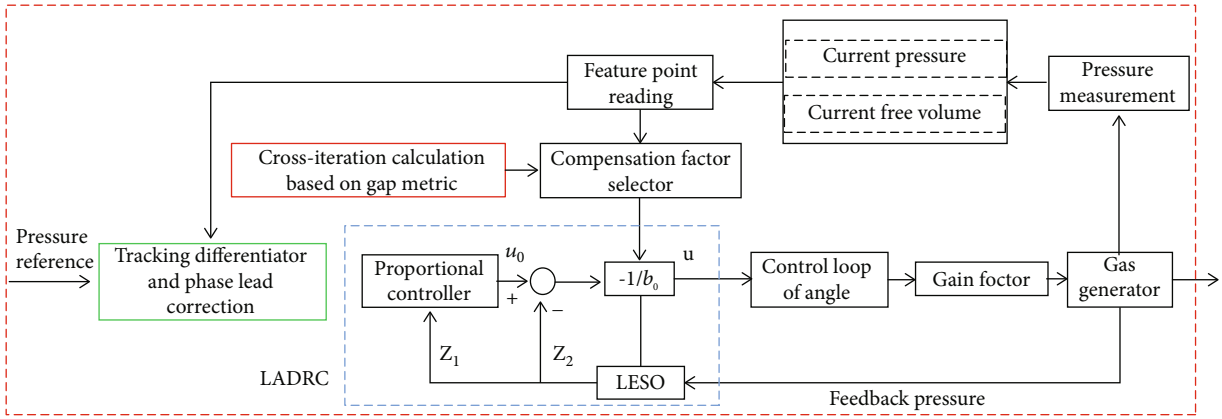

Figure 13: Principle of GM-LADRC.

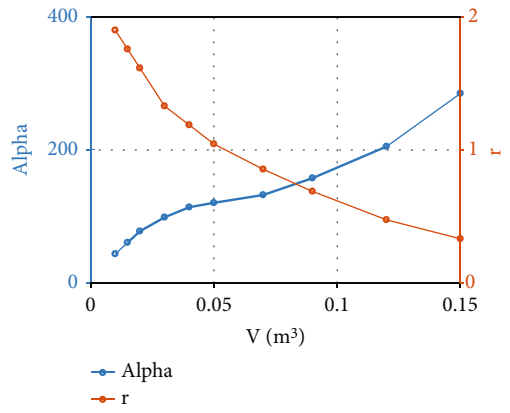

Figure 14: The regulation law of α and r with free volume.

Table 1: Simulation conditions.

GG model parameters	Value (unit)	GM-LADRC's parameters	Value
A_b	0.0924 m^2	ω_c	10
a	0.0063 m/s	h	0.01
n	0.53	K	5
ρ_b	1630 kg/m^3	b_0 (1, 1)	2

when $j = 1$, $b_0(i, j)$ is uniquely determined by $b_{P_g}(i, j)$. Here, $b_0(i, j)$ is the compensation factor "b_0" in equation (10). GAP_{P_g} denotes the gap between adjacent set points when the free volume is constant but the pressure varies, and GAP_V denotes the gap between the adjacent set points when the pressure is constant but the free volume varies. Definition K is the gap factor, which is always constant. The adaptivity of the control law was ensured by the variation of the gap and the compensation factor.

The computational process expressed in equation (18) could be more visually represented in Figure 10, where each blue "box" represents a compensation factor cell to be calculated cross-iteratively, each cell being determined jointly by GAP_{P_g} and GAP_V. After the calculation, the compensation factors in the neighboring boxes were calculated in the same way; based on the variation of the zero position, the monotonic variation of b_0 should be ensured as much as possible. The present method only needs to adjust the gap factor K, in the whole nonlinear domain, while the traditional method needs to adjust compensation factor based on each set point. For example, this system was divided into 100 set points, and then, the traditional way needs to tune 100 compensation factors. Eventually, the calculation results of compensation

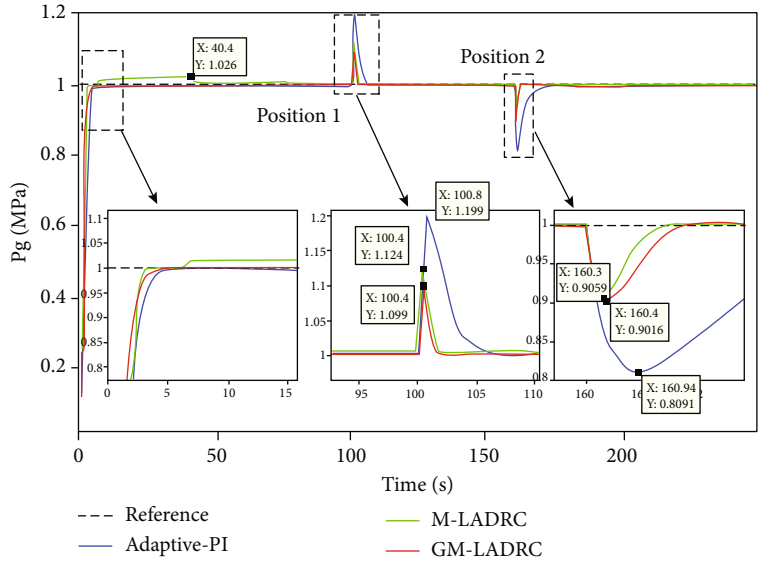

Figure 15: Step response of pressure under external disturbance.

factor according to the above method are shown in Figure 11.

As mentioned earlier, after introducing the valve motor model, the stability of the system needs to be reassessed. After examining the stability of the "base point" (Figure 9), we also select the set point at $P_g = 4.48$ MPa and $V = 0.15$ m^3 for stability analysis. As shown in Figure 12, it can be judged that the stability condition of the system at this set point is $b_0 > 1/18.7$, while the stability condition at the "base point" is $b_0 > 1/5.68$. Since the multilinear model of the system showed a clear regularity in the change of the zero position, it can be roughly deduced that the value of b_0, which makes the system critically stable at each set point, decreases gradually with the increase of the gas pressure and free volume. Therefore, b_0 mapped by the gap metric in Figure 11 all satisfy the stability requirement, where $b_0(10, 10)$ is about 5.5 and the overshoot near this set point is about 35%, which can be reduced by equation (19).

5. LADRC's Principle for Multilinear Model of Gas Flow Regulation System

The principle of controller is shown in Figure 13. The compensation factor selector makes a set point judgment based on the feedback pressure value and interpolates a real-time b_0 value from a library of compensation factor calculated by the gap metric. The LADRC has three inputs, the "processed" pressure command signal, the feedback value of the GG pressure, and the updated value of the compensation factor. The output is the control amount of the valve angle. The LADRC based on gap metric designed in this paper denoted as "GM-LADRC."

In this control law design process, the preprocessing of the pressure command can be described as equation (19), which has the function of softening the input signal and

Table 2: Deviations corresponding to various internal disturbances.

Deviation conditions	a	C_r	n
Normal condition	+0%	+0%	+0%
1	+10%	+15%	−10%
2	+10%	−15%	+10%

phase overcorrection. It corresponds to the part surrounded by the green box in Figure 13.

$$\begin{cases} fh = r^2 \bullet (C - x_1(k)) - 2 \bullet r \bullet x_2(k), \\ x_1(k+1) = x_1(k) + h \bullet x_2(k), \\ x_2(k+1) = x_2(k) + h \bullet fh, \\ R = x_1(k+1) + h \bullet \alpha \bullet x_2(k+1), \end{cases} \tag{19}$$

where C represents the pressure reference, R is the output of this module, and h is the step size. α and r are the parameters to be tuned (α = alpha), whose value varies monotonically with the free volume during the design of this control law, as shown in Figure 14.

6. Simulation-Based Quantitative Analysis of Multivariate Metrics

It is also important to note that the M-LADRC does not need to tune compensation factors too; for linear systems, M-LADRC allows it to converge faster in the presence of disturbances than traditional LADRC methods; the model-assisted ESO (M-ESO) could be written in the form of equation (20) [38]. In order to analyze the performance of GM-LADRC, this paper compared it with the adaptive PI controller and M-LADRC. For the consideration of undershoot,

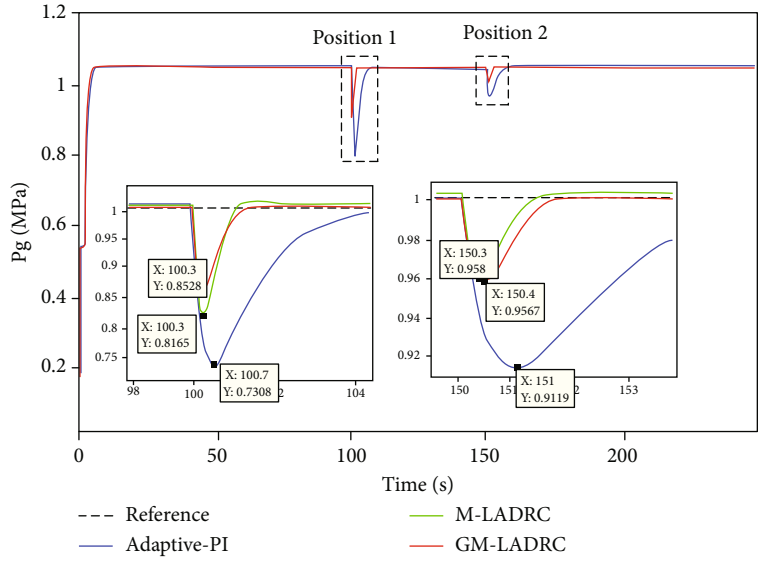

Figure 16: Step response of pressure under internal disturbance.

Table 3: Maximum deviation of the pressure response.

Form of disturbance	Position	Adaptive PI	M-LADRC	GM-LADRC
External disturbance	Position 1	0.1990 MPa	0.1240 MPa	0.0990 MPa
	Position 2	0.1909 MPa	0.0941 MPa	0.0984 MPa
Internal disturbance	Position 1	0.2692 MPa	0.1835 MPa	0.1472 MPa
	Position 2	0.0881 MPa	0.0420 MPa	0.0434 MPa

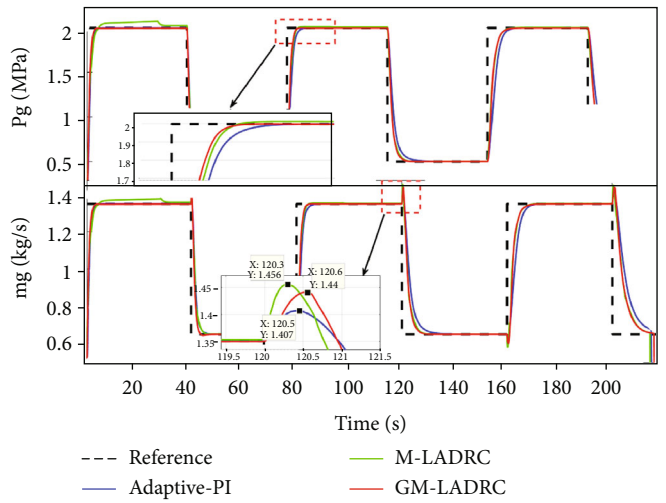

Figure 17: The pressure and gas flow response under square wave signal.

all three controllers described in this paper preprocessed the pressure command with the assistance of equation (19). Matlab/Simulink was used as the simulation software, and the simulation conditions are given in Table 1.

$$\begin{cases} \dot{z}_1 = l_1 \cdot (y - z_1) + z_2 - K_1 \cdot u, \\ \dot{z}_2 = l_2 \cdot (y - z_1) - T_1 \cdot z_2 + K_1 \cdot T_1 \cdot u, \end{cases} \tag{20}$$

where

$$\begin{cases} l_1 = 2 \cdot \omega_0 - T_1, \\ l_2 = (\omega_0 - T_1)^2. \end{cases} \tag{21}$$

Since the ablation of the interstage valve, the deposition of particles in the molten state, and the change of the load torque all eventually lead to the change of the gain factor

Table 4: Scoring of each indicator of the three control laws.

Control law	Disturbance rejection ability	Rapidity	Accuracy	Small overshoot	Total
GM-LADRC	4.4	2.2	1.0	1.0	8.6
M-LADRC	4.6	4.9	4.4	5.0	18.9
Adaptive-PI	1.0	2.3	5.0	5.0	13.3

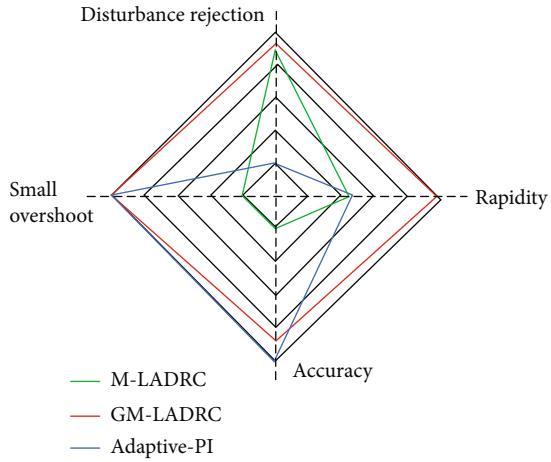

Figure 18: Comparison of the advantages and disadvantages of the three control laws.

from the motor output angle to the throat area, the gain factor was made to change from 1 to 0.9 at the 100th second and from 0.9 to 1 at the 160th second in the simulation to reflect the uncertainty change of the valve as well as the load. As depicted in Figure 15, the disturbance rejection ability of GM-LADRC and M-LADRC was relatively close, with a maximum fluctuation of about 0.1 MPa, but the M-LADRC caused a maximum overshoot of about 5%. The adaptive PI controller had the worst disturbance rejection ability, with a maximum fluctuation of about 0.2 MPa caused by a change in the gain factor. The adaptive PI control law had the best steady-state accuracy, followed by the GM-LADRC.

If the above changes to the gain coefficients could be considered as external disturbance, then next we would make deviations to the internal parameters of the system in order to study the performance of the three controllers under the internal disturbance of the system. When the pressure command was constant at 1 MPa, we made the system maintain the standard condition for the first 100 seconds, and at the 100th second, the deviation was generated for the three parameters inside the system according to no. 1 (in Table 2), which continued until the 150th second when it became the deviation corresponding to no. 2 (in Table 2), as shown in Table 2. The response results are shown in Figure 16, and it could be seen that the best performance still belonged to the GM-LADRC, and the maximum deviation of the pressure response is counted in Table 3.

Figure 17 shows that the response of the gas flow had different degrees of undershoot due to the NMP characteristic of the pressure-to-gas flow response process. The adaptive PI controller had the smallest undershoot due to its slowest response, and the undershoot of the remaining two control laws was comparable, with GM-LADRC being slightly smaller than M-LADRC at 13% and adaptive PI at about 6.5%. After about 214 seconds, the propellant was burned out.

The above simulation results had shown that each of the three control laws had its own advantages and disadvantages. In order to obtain the comprehensive performance of each control law in more dimensions, the four indexes of " disturbance rejection ability," "rapidity," "accuracy," and "overshoot" of the three control laws were "scored," respectively.

The scoring method [39] was carried out according to equation (22), and the simulations were tested from the lowest pressure response to $[0.6,2.5]$ MPa in the method shown in Figures 15 and 16, respectively. For a total of 40 sets of simulations (20 groups each for internal disturbance simulation and external disturbance simulation), the final score was taken as the average score of the 40 sets of simulation results. The results are shown in Table 4, and finally, "GM-LADRC" won the highest score, indicating that it had the best overall performance. Figure 18 is a more visual depiction of it. (See Tables S1–S6 in Supplementary Materials for score analysis.)

$$\mathrm{Sco} = \frac{1}{n} \bullet \sum_{i=1}^{n} \left[5 - 4 \bullet \left(\frac{x_j - \min\left(x_j\right)}{\max\left(x_j\right) - \min\left(x_j\right)} \right) \right], \quad \mathrm{Sco} \in [1,5], j \in [1,3], \tag{22}$$

where x_j are the control indexes of the three control laws under the same instruction and simulation conditions and $\max\left(x_j\right)$ is the maximum value of the control index of the three control laws. n is the total number of simulation experiments, and n is 80 because two observed points were set for the "disturbance rejection ability.". For the rest of the indicators, n is 40.

7. Conclusion

In this paper, the GM-LADRC control law was designed for the gas flow regulation problem of SDR. Based on the multilinear model divided by the gap metric method, the gap factor K was introduced, and the compensation factor in the whole operation area was mapped by the gap metric of adjacent set points. According to this method, the parameter tuning of LADRC could be greatly simplified. Compared with the adaptive PI controller, this method still maintained the strong disturbance rejection ability of LADRC, while compared with M-LADRC this method ensured better adaptability to the system and higher control accuracy. In addition, the method described in this article is suitable for systems with strong nonlinearity but little difference in the control bandwidth requirements of the set points. Otherwise, the parameters to be mapped in the LADRC will

increase, which will also increase the difficulty of parameter tuning.

However, when the LADRC method as described in this paper was used for gas flow regulation in SDR, the steady-state error did not converge strictly to zero, or the error converged to zero very slowly; further research is needed for this problem. In addition, on the base of the LADRC frame described in this article, in view of the SDR model uncertainty and actuator dead zone, the use of intelligent algorithms for further online compensation is also a direction worthy of future studies.

Data Availability

Data used to support the findings of this study are available from the corresponding author upon request.

Conflicts of Interest

The authors declare that there is no conflict of interest regarding the publication of this paper.

Acknowledgments

I would like to show my deepest gratitude to my supervisor, Dr. Zeng Qinhua, a respectable and resourceful scholar, who has provided me with valuable guidance in every stage of the writing of this thesis. This research is financially supported by the National Natural Science Foundation of China (Grant No. 61174120).

Supplementary Materials

The detailed derivation process of equations (2) and (3) was supplemented in part A, equation (11)'s was supplemented in part B, and equation (12)'s was supplemented in part C of the supplementary materials. In addition, we provide 20 sets of simulation results for each of the three control laws under internal disturbance, as shown in Tables S1–S3. And we also provide 20 sets of simulation results for each of the three control laws under external disturbance, as shown in Tables S4–S6. *(Supplementary Materials)*

References

[1] Z. X. Xia, B. B. Chen, L. Y. Huang, D. Wang, and L. Ma, "Research progresses in solid rocket-ramjet engine," *Aerospace Shanghai*, vol. 36, no. 6, pp. 11–18, 2019.

[2] W. Y. Niu, W. Bao, J. T. Chang, T. Cui, and D. R. Yu, "Control system design and experiment of needle-type gas regulating system for ducted rocket," *Proceedings of the Institution of Mechanical Engineers, Part G: Journal of Aerospace Engineering*, vol. 224, no. 5, pp. 563–573, 2010.

[3] J. T. Chang, B. Li, W. Bao, W. Niu, and D. Yu, "Thrust control system design of ducted rockets," *Acta Astronautica*, vol. 69, no. 1-2, pp. 86–95, 2011.

[4] J. T. Chang, B. Li, W. Bao, W. Niu, and D. Yu, "Friction-compensation control of gas-flow regulation for ducted rockets based on adaptive dither method," *Journal of Aerospace Engineering*, vol. 26, no. 4, pp. 715–720, 2013.

[5] A. Alan, Y. Yildiz, and U. Poyraz, "Adaptive pressure control experiment: controller design and implemen-tation," in *IEEE conference on control technology and applications*, pp. 27–30, Hawai'i, August 2017.

[6] A. Wang and Q. H. Zeng, "Load characteristics and modeling methods for the flow regulator of a solid ducted rocket," *International Journal of Aerospace Engineering*, vol. 2019, Article ID 8031290, 10 pages, 2019.

[7] R. Zhou, C. F. Fu, and W. Tan, "Implementation of linear controllers via active disturbance rejection control structure," *IEEE Transactions on Industrial Electronics*, vol. 68, no. 7, pp. 6217–6226, 2021.

[8] G. Herbst, "Transfer function analysis and implementation of active disturbance rejection control," *Control Theory and Technology*, vol. 19, no. 1, pp. 19–34, 2021.

[9] H. X. Zhuang, Q. L. Sun, Z. Q. Chen, and X. Zeng, "Active disturbance rejection control for attitude control of missile systems based on back-stepping method," *International Journal of Control, Automation and Systems*, vol. 19, no. 11, pp. 3642–3656, 2021.

[10] J. J. Chen, J. Q. Wang, Y. X. Liu, and Z. Hu, "Design and verification of aeroengine rotor speed controller based on U-LADRC," *Mathematical Problems in Engineering*, vol. 2020, 12 pages, 2020.

[11] Y. Ma, M. Yan, X. Zhou, and J. Yin, "Application of model compensated active disturbance rejection control in electric vehicle charging," in *IEEE International Conference on Mechatronics and Automation*, pp. 570–575, Takamatsu, Japan, August 2021.

[12] Y. T. Wang, W. Tan, W. Q. Cui, W. Han, and Q. Guo, "Linear active disturbance rejection control for oscillatory systems with large time-delays," *Journal of the Franklin Institute*, vol. 358, no. 12, pp. 6240–6260, 2021.

[13] Z. H. Cai, Z. X. Wang, J. Zhao, and Y. Wang, "Equivalence of LADRC and INDI controllers for improvement of LADRC in practical applications," *ISA Transactions*, vol. 7, 2021.

[14] W. Cui, W. Tan, D. Li, Y. Wang, and S. Wang, "A relay feedback method for the tuning of linear active disturbance rejection controllers," *IEEE Access*, vol. 8, no. 1, pp. 4542–4550, 2020.

[15] C. F. Fu and W. Tan, "Parameters tuning of reduced-order active disturbance rejection control," *IEEE Access*, vol. 8, no. 4, pp. 72528–72536, 2020.

[16] X. Chen and D. Z. Li, "Study on characteristic model based linear active disturbance rejection controller for a class of nonlinear systems," *33rd Chinese Control and Decision Conference*, 2021, pp. 2167–2172, Kunming, China, May 2021.

[17] B. Zhang, B. Wang, Z. Yao, and C. Tang, "Linear active disturbance rejection control for propeller-driving system based on model information compensation," in *2020 39th Chinese Control Conference (CCC)*, pp. 3538–3543, Shenyang, China, July 2020.

[18] Z. G. Wang, C. Y. Yu, M. J. Li, B. Yao, and L. Lian, "Vertical profile diving and floating motion control of the underwater glider based on fuzzy adaptive LADRC algorithm," *Journal of Marine Science and Engineering*, vol. 9, no. 7, article 698, 2021.

[19] Y. S. Fan, L. Lei, and Y. Yu, "ADRC course control for USV based on fuzzy self-tuning," in *2021 4th International Conference on Intelligent Autonomous Systems*, pp. 307–311, Wuhan, China, May 2021.

[20] H. Zhang, Y. Wang, G. Zhang, and C. Tang, "Research on LADRC strategy of PMSM for road-sensing simulation based

on differential evolution algorithm," *Journal of Power Electronics*, vol. 20, no. 4, pp. 958–970, 2020.

[21] D. Li, X. Chen, J. Zhang, and Q. Jin, "On parameter stability region of LADRC for time-delay analysis with a coupled tank application," *Processes*, vol. 8, no. 2, article 223, 2020.

[22] Z. G. Wang, Z. C. Lyu, and J. B. Li, "Parameter tuning of active disturbance rejection control in quad tilt rotor based on particle swarm optimization," *Journal of Physics: Conference Series*, vol. 1780, article 012023, 2021.

[23] F. Yang, K. Wang, M. Zhang, Y. Dai, Z. Pan, and M. Sun, "Parameters tuning and optimization of linear active disturbance rejection control subject to actuator rate limit," in *2020 7th International Conference on Information Science and Control Engineering*, pp. 2002–2006, Changsha, China, Dec 2020.

[24] G. Hou, L. Gong, M. Wang, X. Yu, Z. Yang, and X. Mou, "A novel linear active disturbance rejection controller for main steam temperature control based on the simultaneous heat transfer search," *ISA Transactions*, vol. 122, pp. 357–370, 2022.

[25] Q. H. Ouyang, K. G. Fan, Y. H. Liu, and N. Li, "Adaptive LADRC parameter optimization in magnetic levitation," *IEEE Access*, vol. 9, no. 3, pp. 36791–36801, 2021.

[26] B. W. Zhang, W. Tan, and J. Li, "Tuning of linear active disturbance rejection controller with robustness specification," *ISA Transactions*, vol. 85, pp. 237–246, 2019.

[27] C. Q. Liu, G. G. Luo, Z. Chen, and W. Tu, "Measurement delay compensated LADRC based current controller design for PMSM drives with a simple parameter tuning method," *ISA Transactions*, vol. 101, no. 1, pp. 482–492, 2020.

[28] W. Tan and J. H. Xu, "Damping of low-frequency oscillations via active disturbance rejection control," *Electric Power Components and Systems*, vol. 49, no. 3, pp. 233–245, 2021.

[29] Z. Q. Gao, S. H. Hu, and F. J. Jiang, "A novel motion control design approach based on active disturbance rejection," in *Proceedings of the Conference on Decision and Control*, vol. 40, pp. 4877–4882, Orlando, FL, USA, Dec 2001.

[30] Z. Q. Gao, "Scaling and parameterization based controller tuning," *Proceedings Of The American Control Conference*, vol. 6, pp. 4989–4996, 2003.

[31] Z. Q. Chen, Y. Cheng, M. W. Sun, and Q. Sun, "Surveys on theory and engineering applications for linear active disturbance rejection control," *Information and Control*, vol. 46, no. 3, pp. 257–266, 2017.

[32] J. J. Du, C. Y. Song, and P. Li, "Application of gap metric to model bank determination in multilinear model approach," *Journal of Process Control*, vol. 19, no. 2, pp. 231–240, 2009.

[33] K. Hariprasad, S. Bhartiya, and R. D. Gudi, "A gap metric based multiple model approach for nonlinear switched systems," *Journal of Process Control*, vol. 22, no. 9, pp. 1743–1754, 2012.

[34] W. Tan, H. J. Marquez, T. W. Chen, and J. Liu, "Multimodel analysis and controller design for nonlinear processes," *Computers and Chemical Engineering*, vol. 28, no. 12, pp. 2667–2675, 2004.

[35] A. Wang, Q. H. Zeng, L. K. Ma, and H. Wang, "Virtual free-volume revised method and adaptive control for solid ducted rockets," *Journal of Aerospace Engineering*, vol. 34, no. 5, article 04021053, 2021.

[36] T. T. Georgiou and M. C. Smith, "Optimal robustness in the gap metric," *IEEE Transactions on Automatic Control*, vol. 35, no. 6, pp. 673–686, 1990.

[37] D. Yuan, X. J. Ma, Q. H. Zeng, and X. Qiu, "Research on frequency-band characteristics and parameters configuration of linear active disturbance rejection control for second-order systems," *Control Theory & Applications*, vol. 30, no. 12, pp. 1630–1640, 2013.

[38] B. Zhu and F. Yin, *The Core Algorithm of ADRC, Introduction to Active Disturbance Control*, Beijing University of Aeronautics and Astronautics Press, Beijing, 2017.

[39] B. Fu and D. Y. Fang, "A study on the application of radar plot method in comprehensive evaluation," *Statistics & Decision*, vol. 24, pp. 176–178, 2007.